A Method for Controlling Desired Power Received by Multiple Buck Converters in Dynamic Wireless Power Transfer of Multiple Power Receiving Systems

Ryota Kojima
Faculty of Science and Technology
Tokyo University of Science
Noda, Japan
kojima.ryota24@gmail.com

Yusuke Sato
Faculty of Science and Technology
Tokyo University of Science
Noda, Japan

Takehiro Imura
Faculty of Science and Technology
Tokyo University of Science
Noda, Japan

Yoichi Hori
Faculty of Science and Technology
Tokyo University of Science
Noda, Japan

***Abstract*— The power received in multiple-input multiple-output wireless power transfer during driving is highly pulsatile, and it is necessary for the power receiving system alone to be able to suppress the power pulsation. Therefore, we theorize a method to match the received power with the desired power while minimizing the copper loss generated in the receiving coil and propose it as a desired power control method. The proposed method is realized by connecting a buck converter to each power receiving system and making full use of the degree of freedom of its duty ratio. Simulation confirmed that the power control of the proposed method can reduce the pulsation rate of the received power to the desired power by 42.6 points compared to no control.**

Keywords*— *Dynamic Wireless Power Transfer, DWPT, MIMO , Power Control, Buck Converter

I. INTRODUCTION

In recent years, electric vehicles (EVs) have been promoted to achieve carbon neutrality, one of the items of the SDGs. However, problems such as EVs' short cruising range, long recharging time, and battery weight have hindered their widespread use [1]. As a means of solving this problem, DWPT(Dynamic Wireless Power Transfer) is attracting attention; DWPT is a technology for supplying power wirelessly to EVs while driving, and research for passenger cars is already widely underway [2]. There are also studies on DWPT systems for heavy-duty vehicles that have already achieved high power supply [3], [4], [5]. In DWPT for heavy-duty vehicles, it is more economically rational and compatible with existing research to share the same feeder path with passenger cars, which have a relatively small power scale. Therefore, there is a need to construct a power receiving system for large vehicles that increases the power received by using multiple power receiving coils for passenger cars [6].

There are many studies of multiple-input multiple-output (MIMO) WPT systems, and their power characteristics have been revealed [7], [8]. The power characteristics in MIMO DWPT systems are highly pulsating in the total power received [9]. A large capacitor could be placed in front of the battery for smoothing, but providing a buffer to match the power requirements of a large vehicle would require a very large capacity, which would increase weight, volume, and cost. Therefore, it is necessary to construct a system that can control the power received only by the power receiving system in a MIMO DWPT. It is also necessary to consider that the total copper loss generated by the power receiving coils in a power receiving system using multiple power receiving coils is larger than in a single power receiving system.

In this paper, a circuit in which a power receiving coil, a resonant circuit, a rectifier, and a DC/DC converter are connected in series is called a power receiving system. In this paper, we theorize the control that matches the received power with the desired power in a multiple power receiving system as proposed method 1, and the control that minimizes copper loss in the receiving coils while matching the received power with the desired power as proposed method 2. These two proposed methods are realized by making full use of the duty ratio degrees of freedom of each buck converter. Furthermore, the two proposed methods are executed independently in the receiving system and do not require information communication from the transmission side.

II. THEORY

A. Double-LCC Topology

In WPT, the transmission power and efficiency can be greatly improved by utilizing the resonance phenomenon [10]. The schematic shown in Fig. 1(a) is a resonant circuit called Double-LCC circuit, which is employed in this paper [11]. If the angular frequency of the power supply is ω_0 , the resonance condition of the Double-LCC circuit is expressed as in equation (1). The input current I_{in} and output current I_{out} are expressed as in equation (2).

$$\omega_0 = \frac{1}{\sqrt{L_{\mathrm{T0}}C_{\mathrm{Tp}}}} = \sqrt{\frac{C_{\mathrm{Tp}}+C_{\mathrm{Ts}}}{L_{\mathrm{T}}C_{\mathrm{Tp}}C_{\mathrm{Ts}}}} = \frac{1}{\sqrt{L_{\mathrm{R0}}C_{\mathrm{Rp}}}} = \sqrt{\frac{C_{\mathrm{Rp}}+C_{\mathrm{Rs}}}{L_{\mathrm{R}}C_{\mathrm{Rp}}C_{\mathrm{Rs}}}} \quad (1)$$

$$I_{\mathrm{in}} = \frac{MI_{\mathrm{R}}}{L_{\mathrm{T0}}}, \qquad I_{\mathrm{out}} = \frac{MI_{\mathrm{T}}}{L_{\mathrm{R0}}} \quad (2)$$

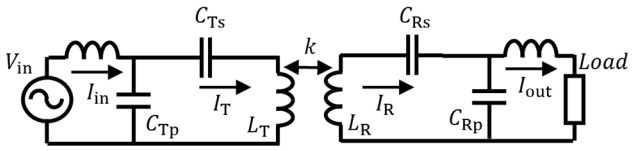

(a) Circuit diagram

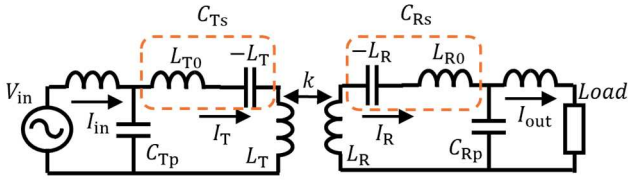

(b) Gyrator exploded view

Fig. 1. Double-LCC Circuit

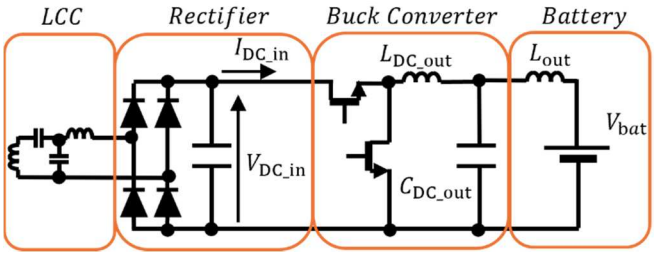

Fig. 2. Receiver side circuit diagram with buck converter

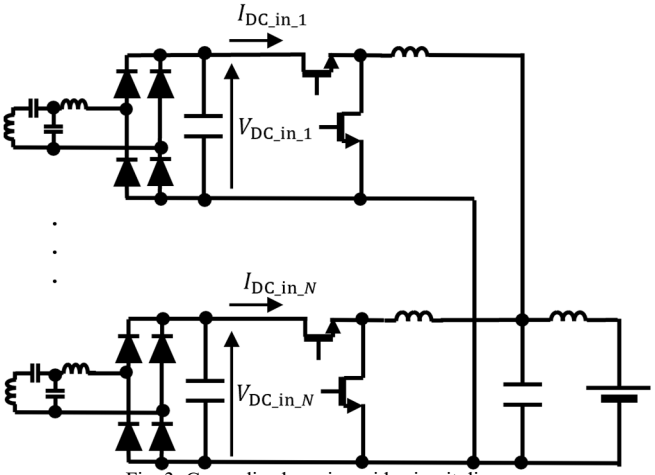

Fig. 3. Generalized receiver side circuit diagram

When the schematic is decomposed as shown in Fig. 1(b), the gyrator circuit composed of L_{T0} and C_{Tp}, L_{R0} and C_{Rp} have the characteristic of interchanging the constant voltage and constant current characteristics of both terminal pairs. As a result, the constant-current characteristics appear in the transmitting and receiving coils in a double-LCC circuit with a constant-voltage power supply and a constant-voltage load connected, providing robustness against resonance misalignment. Similarly, since constant current characteristics appear on the output side, the power received can be controlled by a simple operation of changing the power receiving voltage using a DC/DC converter in the case of a constant-voltage load. In addition, research has shown that the output power characteristics of Double-LCC circuits are less affected by the cross-coupling (CC) phenomenon than those of S-S circuits [9]. The above characteristics are very advantageous for the control of power received, which is the main reason why the Double-LCC circuit is used in this paper.

B. *Buck Converter*

The circuit diagram shown in Fig. 2 represents the power receiving circuit configuration assumed in this paper in the form of a single power receiving system. Since the output side of the resonant circuit has a constant current characteristic, the received current I_{DC_in} is a constant current. As a result, a constant current continues to flow to the smoothing capacitor placed at the rear of the rectifier to fulfill the function of boosting the voltage. Therefore, a buck converter is employed as the DC/DC converter to control the received voltage V_{DC_in}. Assuming the buck converter is ideal, the received voltage V_{DC_in} is determined by equation (3). Since the ON duty ratio d of the high-side MOSFET can be controlled in the range of $0 < d \leq 1$ and the received voltage V_{DC_in} can be set to a value higher than the battery voltage V_{bat}, using a buck converter is more effective than using a boost converter to increase the power received.

$$V_{DC\_in} = \frac{V_{bat}}{d} \tag{3}$$

III. METHOD

A. *System Configuration*

The power receiving circuit configuration assumed in this paper is a power receiving circuit with N power receiving systems connected in parallel to a single battery, as shown in Fig. 3. The received power P_{out} in this power receiving circuit is expressed as in equation (4). Since the output side of the resonant circuit is constant current characteristic, the received currents $I_{DC\_in\_1}$, $I_{DC\_in\_2}$, $\cdots$, $I_{DC\_in\_N}$ in equation (4) are constants proportional to the coupling coefficient. The received voltages $V_{DC\_in\_1}, V_{DC\_in\_2}, \cdots, V_{DC\_in\_N}$ are variables that can be controlled by adjusting the duty ratio d of the buck converter. Therefore, the two proposed methods are realized by calculating the received voltages $V_{DC\_in\_1}$, $V_{DC\_in\_2}$, $\cdots$, $V_{DC\_in\_N}$ that satisfy the control objectives of the two proposed methods and using these as the received voltage command values $V_{ref\_in\_1}, V_{ref\_in\_2}, \cdots, V_{ref\_in\_N}$.

$$P_{out} = \sum_{j=1}^{N} I_{DC\_in\_j} V_{DC\_in\_j} \tag{4}$$

B. *Theoretical Development of the Proposed Method*

This paper proposes two methods to control the received power. The control goal of the proposed method 1 is to match the received power P_{out} with the desired power P_{ref}. The control goal of the proposed method 2 is to minimize the copper loss P_{loss} generated in the receiving coil while keeping the received power P_{out} equal to the desired power P_{ref}. As in the proposed method 1, if the goal is only to control the received power, the ratio of each received voltage $V_{DC\_in\_1}, V_{DC\_in\_2}, \cdots, V_{DC\_in\_N}$ is free. In the proposed method 2, the copper loss of the power receiving coil is reduced by making full use of the degree of freedom of the ratio of each receiving voltage, and the system is designed to reduce the loss during power transmission as much as possible.

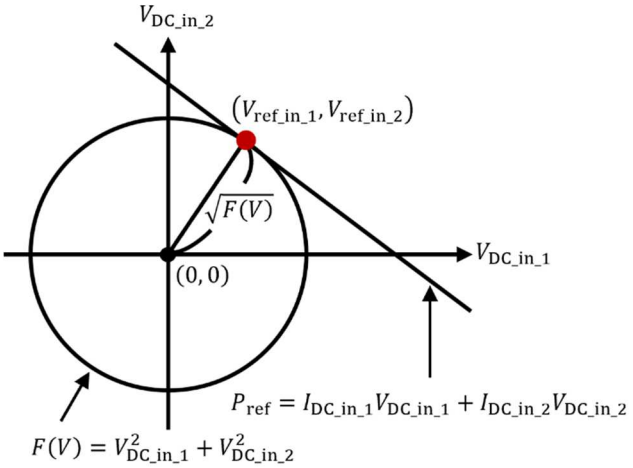

Fig. 4. Approximate form of the evaluation function

This section describes the methods to achieve the proposed method 1 and method 2. The first control goal is to match the received power P_{out} with the desired power P_{ref}. This can be achieved by setting all power receiving voltages $V_{\mathrm{DC\_in\_1}}$, $V_{\mathrm{DC\_in\_2}}$, $\cdots$, $V_{\mathrm{DC\_in\_}N}$ to satisfy equation (5). The second control goal is to minimize the copper loss P_{loss} generated in the power receiving coil. If the internal resistance of the power receiving coil is r_{R} and the current flowing in the receiving coil is I_{R}, the copper loss is expressed as in equation (6). Due to the gyrator characteristics of the resonant circuit, the current I_{R} flowing in the power receiving coil and the voltage $V_{\mathrm{DC\_in}}$ are proportional. Therefore, the magnitude of copper loss P_{loss} is proportional to the square of the receiving voltage $V_{\mathrm{DC\_in}}$. The function $F(V)$, which is expressed as the sum of the squares of the receiving voltages of all N receiving systems as in equation (7), is an evaluation function that expresses the magnitude of the copper loss P_{loss} of the receiving coil. From the above, in the proposed method 1, the voltage that satisfies equation (5) is used as the receiving voltage command value, and in the proposed method 2, the voltage that minimizes $F(V)$ in equation (7) while satisfying equation (5) is used as the receiving voltage command value to achieve each control target.

$$P_{\mathrm{ref}} = \sum_{j=1}^{N} I_{\mathrm{DC\_in\_}j} V_{\mathrm{DC\_in\_}j} \tag{5}$$

$$P_{\mathrm{loss}} = \sum_{j=1}^{N} r_{\mathrm{R\_}j} I_{\mathrm{R\_}j}^2 \tag{6}$$

$$F(V) = \sum_{j=1}^{N} V_{\mathrm{DC\_in\_}j}^2 \tag{7}$$

Calculate the received voltage command values $V_{\mathrm{ref\_in\_1}}$ and $V_{\mathrm{ref\_in\_2}}$ for the proposed method 1 and method 2 for the case $N = 2$. When $N = 2$, equations (5) and (7) are expressed as equations (8) and (9), respectively.

$$P_{\mathrm{ref}} = I_{\mathrm{DC\_in\_1}} V_{\mathrm{DC\_in\_1}} + I_{\mathrm{DC\_in\_2}} V_{\mathrm{DC\_in\_2}} \tag{8}$$

$$F(V) = V_{\mathrm{DC\_in\_1}}^2 + V_{\mathrm{DC\_in\_2}}^2 \tag{9}$$

The control goal of the proposed method 1 can be achieved by satisfying equation (8). The command value of the receiving voltage of the proposed method 1, calculated by a variant of equation (8), is shown in equation (10).

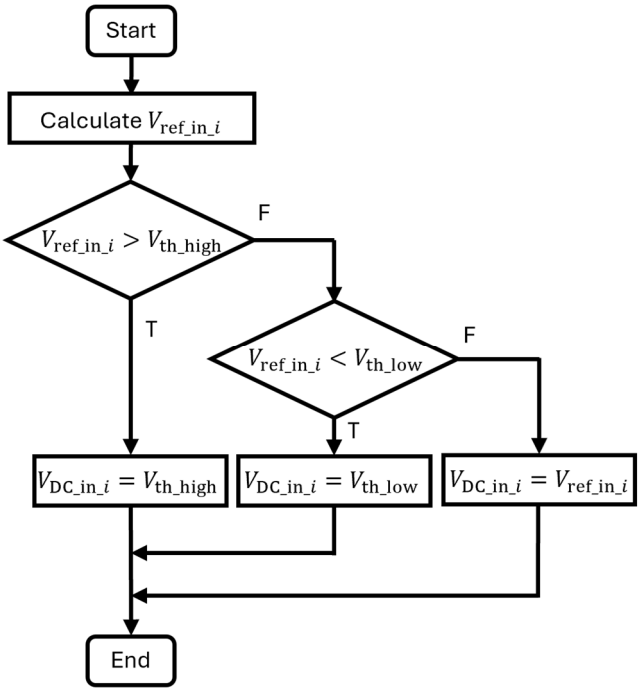

Fig. 5. Control flowchart of proposed method 1

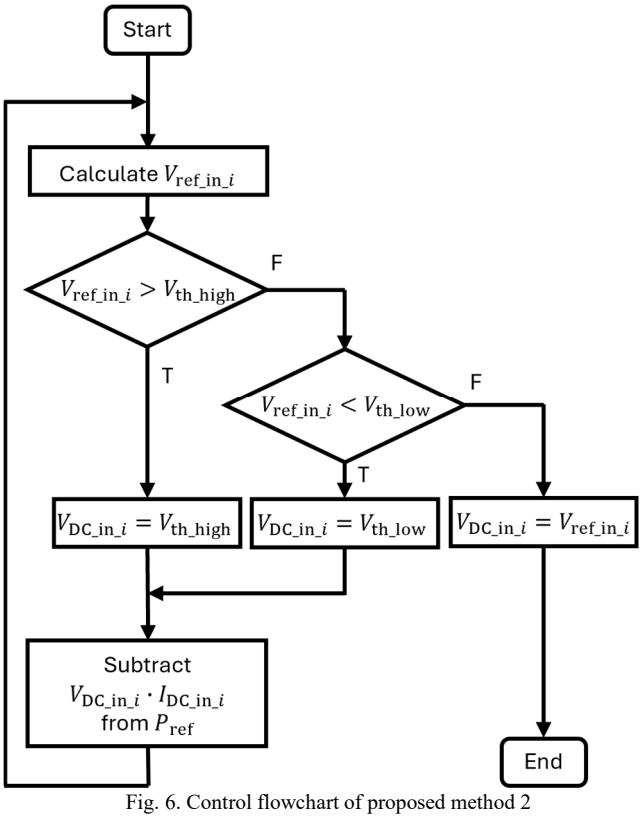

Fig. 6. Control flowchart of proposed method 2

$$V_{\mathrm{ref\_in\_1}} = V_{\mathrm{ref\_in\_2}} = \frac{P_{\mathrm{ref}}}{I_{\mathrm{DC\_in\_1}} + I_{\mathrm{DC\_in\_2}}} \tag{10}$$

The control goal of the proposed method 2 can be achieved by minimizing the $F(V)$ in equation (9) while satisfying equation (8). Assuming a two-dimensional plane with the power receiving voltages $V_{\mathrm{DC\_in\_1}}$ and $V_{\mathrm{DC\_in\_2}}$ as axes, equations (8) and (9) can be illustrated as in Fig. 4, and the $F(V)$ in Fig. 4 is expressed as in equation (11). Since equation (8) must be satisfied for the received power to match the desired power, the point $(V_{\mathrm{ref\_in\_1}}, V_{\mathrm{ref\_in\_2}})$, which points

to the received voltage command value, lies on a straight line. The point on the straight line where $F(V)$ in equation (9) is the smallest is the position with the shortest distance from the origin, which refers to the coordinates of the point of contact between the straight line and the circle. This coordinate can be calculated from the conjunction of equations (8) and (9), and its position for $N = 2$ is expressed as in equation (12).

$$F(V) = \frac{P_{\mathrm{ref}}^2}{I_{\mathrm{DC\_in\_1}}^2 + I_{\mathrm{DC\_in\_2}}^2} \tag{11}$$

$$\begin{cases} V_{\mathrm{ref\_in\_1}} = \dfrac{I_{\mathrm{DC\_in\_1}}}{I_{\mathrm{DC\_in\_1}}^2 + I_{\mathrm{DC\_in\_2}}^2} \cdot P_{\mathrm{ref}} \\ V_{\mathrm{ref\_in\_2}} = \dfrac{I_{\mathrm{DC\_in\_2}}}{I_{\mathrm{DC\_in\_1}}^2 + I_{\mathrm{DC\_in\_2}}^2} \cdot P_{\mathrm{ref}} \end{cases} \tag{12}$$

The case $N = n$ can be calculated in the same way by considering the coordinates of the contact point between an n-dimensional plane and an n-dimensional sphere. Therefore, the received voltage command values $V_{\mathrm{ref\_in}\_i}$ for the i-th power receiving system in the proposed method 1 and method 2 can be generalized as in equations (13) and (14), respectively.

$$V_{\mathrm{ref\_in}\_i} = \frac{P_{\mathrm{ref}}}{\sum_{j=1}^{n} I_{\mathrm{DC\_in}\_j}} \tag{13}$$

$$V_{\mathrm{ref\_in}\_i} = \frac{I_{\mathrm{DC\_in}\_i}}{\sum_{j=1}^{n} I_{\mathrm{DC\_in}\_j}^2} \cdot P_{\mathrm{ref}} \tag{14}$$

The flowcharts in Fig. 5 and Fig. 6 show the flowcharts for determining the receiving voltage of the i-th receiving system in the proposed method 1 and method 2, respectively. The upper and lower limits of the receiving voltage, $V_{\mathrm{th\_high}}$ and $V_{\mathrm{th\_low}}$, are determined arbitrarily according to the system that incorporates this control method.

IV. Simulation Results

A. Environment of the Simulation

The simulation was performed by MATLAB/Simulink. The purpose of the simulation is to confirm the feasibility of the two proposed methods. For the simulation, a system with five transmission coils and three receiving coils was constructed and measured. Therefore, the circuit configuration on the power receiving side is $N = 3$ in Fig. 3, which is a power receiving circuit with three power receiving systems connected in parallel to a single battery. Note that the system has no CC phenomenon between the receiving coils. In the above configuration, simulations were performed for three patterns: no control, proposed method 1, and proposed method 2. No control means that the duty ratios d_1, d_2, and d_3 of the three buck converters are all fixed at 0.45. In this paper, the desired power P_{ref} in the proposed method 1 and method 2 was set to 5 kW in simulations, so the average power received in no control was also adjusted to 5 kW by setting the duty ratio of the buck converters to 0.45. The parameters of the simulation are listed in Table. 1. In the simulation, the coupling coefficients vary as shown in Fig. 7. Fig. 8 shows the simulation results of the received currents $I_{\mathrm{DC\_in\_1}}$, $I_{\mathrm{DC\_in\_2}}$, and $I_{\mathrm{DC\_in\_3}}$ without control. From Fig. 7 and Fig. 8, it can be reconfirmed that the receiving currents $I_{\mathrm{DC\_in\_1}}$, $I_{\mathrm{DC\_in\_2}}$, and $I_{\mathrm{DC\_in\_3}}$ are constants proportional to the coupling coefficient.

Table 1. Simulation parameters

Vehicle velocity	v	20 km/h
DC power supply voltage	V_{in}	600 V
Battery voltage	V_{bat}	120 V
Operation frequency	f	85 kHz
Primary compensated inductance	L_{T0}	49.3 μH
Primary compensated capacitor	C_{Tp}	71.1 nF
Primary resonant capacitor	C_{Ts}	22.4 nF
Primary transmitter inductance	L_{T}	205.8 μH
Secondary compensated inductance	L_{R0}	26.4 μH
Secondary compensated capacitor	C_{Rp}	132.6 nF
Secondary resonant capacitor	C_{Rs}	139.8 nF
Secondary receiver inductance	L_{R}	51.5 μH
Secondary receiver resistance	r_{R}	65 mΩ
Desired power	P_{ref}	5 kW
Buck converter carrier frequency	$f_{\mathrm{DC/DC}}$	50 kHz
Power transmission coil length	l_{T}	500 mm
Power transmission coil spacing	d_{TT}	200 mm
Power receiving coil length	l_{R}	200 mm
Power receiving coil spacing	d_{RR}	50 mm
Buck converter output inductor	$L_{\mathrm{DC\_out}}$	900 μH
Buck converter output capacitor	$C_{\mathrm{DC\ out}}$	300 μF
Inductor before battery	L_{out}	100 μH

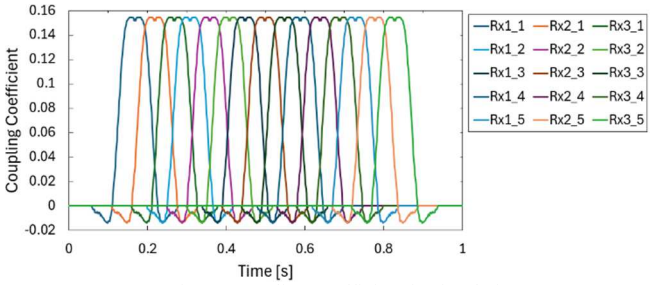

Fig. 7. Coupling coefficient in simulation

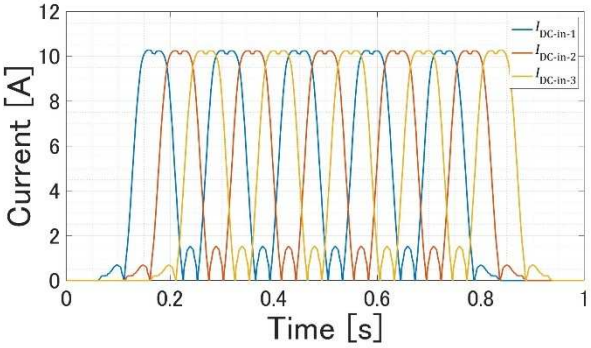

Fig. 8. Simulation results of received current

B. Simulation Results of Power Received

The duty ratio commands d_1, d_2, and d_3 of the three buck converters in the proposed method 1 and method 2 vary as shown in Fig. 9 and Fig. 10, respectively. Fig. 11, Fig. 12, and Fig. 13 show the simulation results of the received power P_{out} for no control, proposed method 1, and proposed method 2, respectively. As an evaluation index of the power control, we use the pulsation rate r_{f} calculated from equation (15). The numerator of equation (15) is the difference between the maximum power P_{MAX} and the minimum power P_{MIN} within the range where the periodicity of power transmission is recognized. In this paper, 0.3 to 0.7 s in the simulation results is considered to be the range where the periodicity of power transmission is recognized. Substitute 5 kW, the desired power in this paper, in the denominator of equation (15). The calculated pulsation rate r_{f} of the received power is shown in Table.2.

$$r_{\mathrm{f}} = \frac{P_{\mathrm{MAX}} - P_{\mathrm{MIN}}(During\ Power\ Transmission)}{Target\ Power} \quad (15)$$

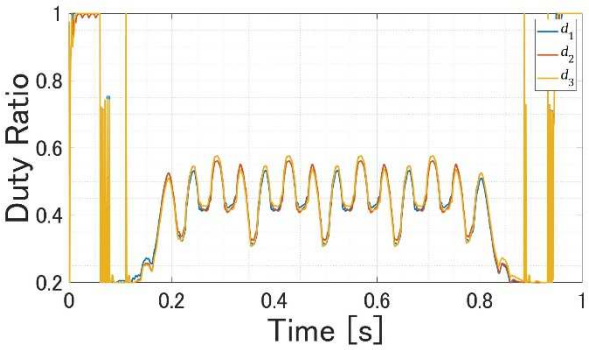

Fig. 9. Duty ratio in proposed method 1

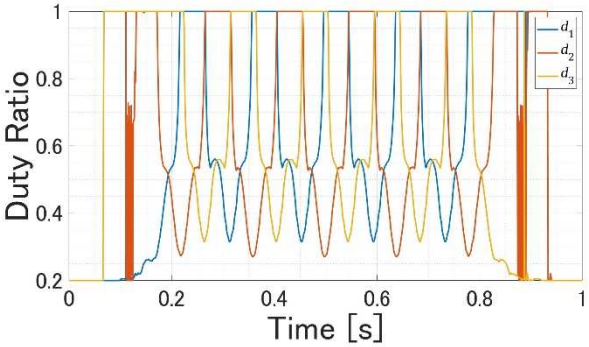

Fig. 10. Duty ratio in proposed method 2

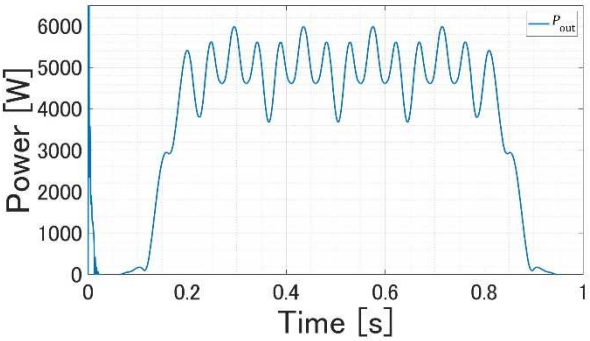

Fig. 11. Received power P_{out} in no control

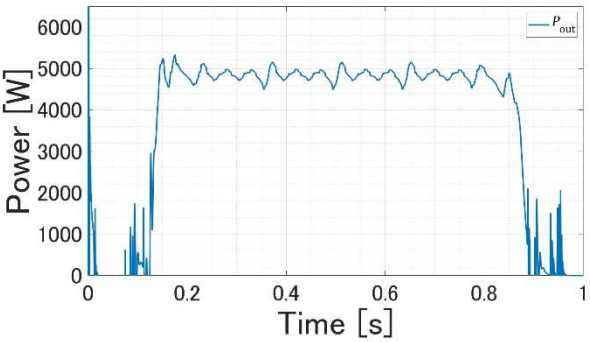

Fig. 12. Received power P_{out} in the proposed method 1

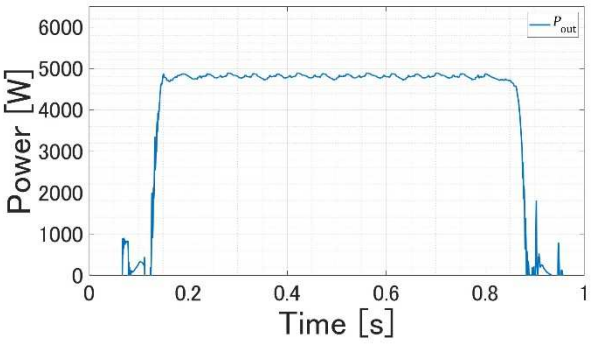

Fig. 13. Received power P_{out} in the proposed method 2

Table 2. Pulse rate of received power P_{out}

	No control	Method 1	Method 2
r_{f} [%]	46.2	13.4	3.6

Table 2 shows that the proposed method 1 reduces the pulsation rate r_{f} by 32.8 points compared to no control, and the proposed method 2 reduces the pulsation rate r_{f} by 42.6 points compared to no control, which confirms that the two proposed methods can control power appropriately. In addition, the pulsation rate r_{f} of the proposed method 2 is reduced by 9.8 points compared to the proposed method 1, indicating that the pulsation rate can be improved by reducing the copper loss. On the other hand, Fig. 12 and Fig. 13 show that the received power P_{out} is slightly lower than the desired power $P_{\mathrm{ref}} = 5$ kW despite the power control. This is because the buck converter is assumed to be ideal in this paper, but in reality power losses occur in the buck converter section.

C. Simulation Results of Copper Loss

Fig. 14, Fig. 15, and Fig. 16 show the simulation results of the copper loss $P_{\mathrm{loss\_1}}$, $P_{\mathrm{loss\_2}}$, and $P_{\mathrm{loss\_3}}$ generated in each receiving coil of the three receiving systems and the total copper loss $P_{\mathrm{loss\_total}}$ represented by the sum of these losses in no control, proposed method 1, and proposed method 2, respectively. The average power $\bar{P}_{\mathrm{loss\_total}}$ of total copper loss $P_{\mathrm{loss\_total}}$ from 0.3 to 0.7 s for no control, proposed method 1, and proposed method 2, respectively, are shown in Table.3.

Table 3 shows that the proposed method 1, which does not consider copper loss reduction, increases the average power by 2.8% compared to no control, while the proposed method 2 reduces the average power by 20.6% compared to no control. The proposed method 2 reduces the average power of copper loss by 10 points compared to proposed method 1, which confirms that the operation to reduce copper loss is properly performed.

These simulation results confirm that the two proposed methods work properly at high voltage scales of 600 V for the transmission voltage and 120 V for the receiving voltage.

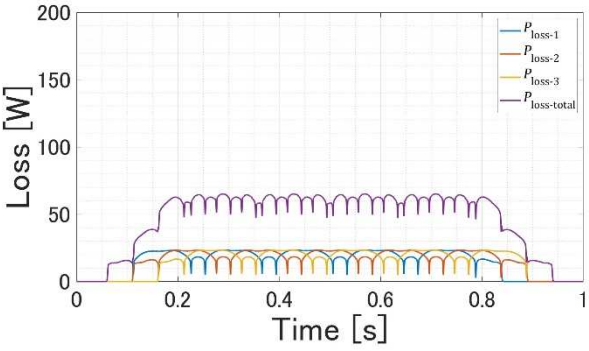

Fig. 14. Copper loss in no control

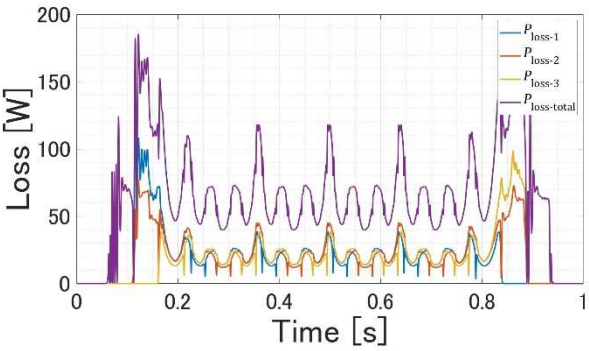

Fig. 15. Copper loss in the proposed method 1

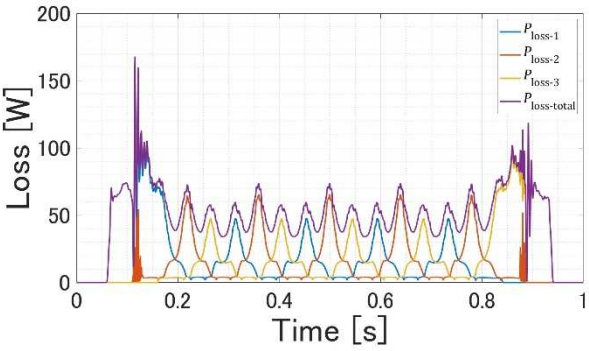

Fig. 16. Copper loss in the proposed method 2

Table 3. Average power of copper loss $P_{\mathrm{loss\_total}}$

	No control	Method 1	Method 2
$\bar{P}_{\mathrm{loss\_total}}$ [W]	61.6	63.3	48.9

V. Conclusion

In this paper, two methods are proposed to control the received power by voltage control using multiple buck converters in a multi-input, multi-output DWPT system. The two proposed methods were verified by simulation using MATLAB/Simulink. The simulation results confirmed that the power control of the proposed method 1 can reduce the pulsation rate of the received power by 32.8 points compared to no control. In addition, the power control using the proposed method 2 can reduce the pulsation rate of the received power by 42.6 points compared to no control, indicating that the pulsation rate can be improved by reducing the copper loss. However, the two proposed methods have power control, yet the power received is slightly below the desired power. This is due to power loss in the buck converter section, which was not assumed in this paper, and we are considering a solution by incorporating feedback control as a future issue.

Acknowledgment

This paper is based on results obtained from a project commissioned by Ministry of Land, Infrastructure, Transport and Tourism (MLIT) in Japan.

References

[1] J. Bi, Y. Wang, Q. Sai, and C. Ding, “Estimating remaining driving range of battery electric vehicles based on real-world data: A case study of Beijing, China,” *Energy*, vol. 169, pp. 833–843, Feb. 2019, doi: 10.1016/j.energy.2018.12.061.

[2] A. Chitta Bagchi, A. Kamineni, R. Andrew Zane, S. Member, and R. Carlson, “Review and Comparative Analysis of Topologies and Control Methods in Dynamic Wireless Charging of Electric Vehicles,” *IEEE J Emerg Sel Top Power Electron*, vol. 9, no. 4, p. 4947, 2021, doi: 10.1109/JESTPE.2021.3058968.

[3] S. Obayashi *et al.*, “85 kHz Band 44 kW Wireless Rapid Charging System for Field Test and Public Road Operation of Electric Bus,” 2019, doi: 10.3390/wevj10020026.

[4] T. Tajima, W. Noguchi, and H. Shigi, “450-kW Conductive Dynamic Charge System,” 2023.

[5] G. Guidi and J. Are Suul, “High power and power density inductive charging system for busses and heavy-duty vehicles,” 2023.

[6] B. J. Varghese *et al.*, “Multi-Pad Receivers for High Power Dynamic Wireless Power Transfer,” *2020 IEEE Energy Conversion Congress and Exposition (ECCE)*, 2020, doi: 10.1109/ECCE44975.2020.9235918.

[7] T. Aoki, Q. Yuan, D. Quang-Thang, M. Okada, H.-M. Hsu, and N. Sentan Kagaku Gijutsu Daigakuin Daigaku, “Maximum Transfer Efficiency of MIMO-WPT System,” in *2018 IEEE Wireless Power Transfer Conference (WPTC)*, 2018, pp. 1–3.

[8] H. Lee and B. Lee, “Investigation of MIMO Wireless Power Transfer Efficiency in Optimization Techniques,” in *2020 IEEE International Symposium on Antennas and Propagation and North American Radio Science Meeting, IEEECONF 2020 - Proceedings*, Institute of Electrical and Electronics Engineers Inc., Jul. 2020, pp. 1417–1418. doi: 10.1109/IEEECONF35879.2020.9330339.

[9] T. Kawakami, T. Imura, and Y. Hori, “Basic Study on the Distance between Receiving Coils for Dynamic Wireless Power Transfer to Heavy Vehicles,” in *Technical Committee on Semiconductor Power Converter IEEJ Industry Applications Society*, Mar. 2022, pp. 29–34.

[10] A. Kurs, A. Karalis, R. Moffatt, J. D. Joannopoulos, P. Fisher, and M. Soljacic, “Wireless Power Transfer via Strongly Coupled Magnetic Resonances,” *Science (1979)*, vol. 317, no. 5834, pp. 83–86, Nov. 2007, doi: 10.1016/j.aop.2007.04.017.

[11] S. Li, W. Li, J. Deng, D. Nguyen, and C. C. Mi, “A Double-Sided LCC Compensation Network and Its Tuning Method for Wireless Power Transfer,” *IEEE Trans Veh Technol*, vol. 64, no. 6, pp. 2261–2273, Aug. 2015, doi: 10.1109/TVT.2014.2347006.